European Journal of Immunology

HIV–TB coinfection impairs CD8$^+$ T-cell differentiation and function while dehydroepiandrosterone improves cytotoxic antitubercular immune responses

Guadalupe V. Suarez[1], Matías T. Angerami[1], María B. Vecchione[1], Natalia Laufer[1,2], Gabriela Turk[1], Maria J. Ruiz[1], Viviana Mesch[3], Bibiana Fabre[3], Patricia Maidana[3], Diego Ameri[2], Pedro Cahn[2,4], Omar Sued[4], Horacio Salomón[1], Oscar A. Bottasso[5] and María F. Quiroga[1]

[1] Instituto de Investigaciones Biomédicas en Retrovirus y SIDA, Universidad de Buenos Aires - CONICET, Argentina
[2] Hospital Juan A. Fernández, Buenos Aires, Argentina
[3] Departamento de Bioquímica Clínica, INFIBIOC, Facultad de Farmacia y Bioquímica, Universidad de Buenos Aires, Argentina
[4] Área de Investigaciones Médicas, Fundación Huésped, Buenos Aires, Argentina
[5] Instituto de Inmunología Clínica y Experimental de Rosario (IDICER), CONICET-UNR, Rosario, Santa Fe, Argentina

Tuberculosis (TB) is the leading cause of death among HIV-positive patients. The decreasing frequencies of terminal effector (T_{TE}) CD8$^+$T cells may increase reactivation risk in persons latently infected with *Mycobacterium tuberculosis (Mtb)*. We have previously shown that dehydroepiandrosterone (DHEA) increases the protective antitubercular immune responses in HIV–TB patients. Here, we aimed to study *Mtb*-specific cytotoxicity, IFN-γ secretion, memory status of CD8$^+$T cells, and their modulation by DHEA during HIV–TB coinfection. CD8$^+$T cells from HIV–TB patients showed a more differentiated phenotype with diminished naïve and higher effector memory and T_{TE} T-cell frequencies compared to healthy donors both in total and *Mtb*-specific CD8$^+$T cells. Notably, CD8$^+$T cells from HIV–TB patients displayed higher Terminal Effector (T_{TE}) CD45RA^{dim} proportions with lower CD45RA expression levels, suggesting a not fully differentiated phenotype. Also, PD-1 expression levels on CD8$^+$T cells from HIV–TB patients increased although restricted to the CD27$^+$ population. Interestingly, DHEA plasma levels positively correlated with T_{TE} in CD8$^+$T cells and in vitro DHEA treatment enhanced *Mtb*-specific cytotoxic responses and terminal differentiation in CD8$^+$T cells from HIV–TB patients. Our data suggest that HIV–TB coinfection promotes a deficient CD8$^+$ T-cell differentiation, whereas DHEA may contribute to improving antitubercular immunity by enhancing CD8$^+$T-cell functions during HIV–TB coinfection.

Keywords: Coinfection · CD8$^+$ T cells · Cell differentiation · DHEA · HIV · Tuberculosis

Additional supporting information may be found in the online version of this article at the publisher's web-site

Introduction

Nearly one-third of the world's population is infected with *Mycobacterium tuberculosis* (*Mtb*), the etiologic agent of tuberculosis (TB). HIV coinfection is the main risk factor for progression

Correspondence: Guadalupe V. Suarez
e-mail: suarez_guadalupe@hotmail.com

from latent to active TB disease, increasing the risk of latent TB (LTB) reactivation up to 20-fold [1].

It is well established that $CD4^+$T cells are critical for resistance to *Mtb* [2]. *Mtb* infection also elicits $CD8^+$T-cell responses, which are recruited to the lung during infection and found in the granulomas of infected people [3]. Although it is still unknown how $CD8^+$T cells may mediate protection against TB, it has been suggested that while $CD4^+$T cells are more important in controlling bacterial replication during the acute phase of infection, $CD8^+$T cells play a greater role during latency, possibly via immune-surveillance of cells with higher numbers of intracellular bacilli [4, 5]. Besides cytokine secretion (IFN-γ and TNF-α), $CD8^+$T cells can induce T-cell-mediated cytotoxicity of infected cells, the major function of these cells [6]. Also, cytotoxic $CD8^+$T cells are able to directly kill intracellular bacteria by releasing granule contents [7]. In fact, mice lacking perforin generally succumb to *Mtb* late during infection, consistent with the relevance of $CD8^+$T cells during chronic or LTB infection [8].

In line with this, TNF-α blockade, which increases TB reactivation considerably in LTB persons, decreases the frequency of *Mtb*-specific terminally differentiated (terminal effectors, T_{TE}) $CD8^+$T cells, underscoring the potential role of this population with the highest cytotoxic potential among $CD8^+$T cells, in *Mtb* control [9, 10]. In this regard, while *Mtb*-specific $CD8^+$T cells in HIV^{neg}-LTB patients are mostly composed of T_{TE} cells ($CCR7^{neg}/CD45RA^+$), less differentiated effector memory T cells (T_{EM}, $CCR7^{neg}/CD45RA^{neg}$) predominate among *Mtb*-specific $CD8^+$T cells in HIV^{neg}-active TB patients [11]. Likewise, it has been recently found that cytokine-producing *Mtb*-specific $CD8^+$T cells from HIV–LTB, but not HIV–TB coinfected patients, also exhibited higher T_{TE} frequencies [12], suggesting a protecting role for $CD8^+$ T-cell terminal differentiation against TB. Also, in a preliminary study, convalescing TB subjects with HIV coinfection exhibited a mild impairment in $CD8^+$ T-cell proliferation and IFN-γ production in response to *Mtb* antigens [13]. To our knowledge, no studies have yet been focused on *Mtb*-specific cytotoxic $CD8^+$ T-cell responses or their memory status on HIV–TB coinfected patients, which is central to understand the increasing susceptibility to TB in HIV-infected patients given the proposed role of cytotoxic responses in LTB reactivation [9] and the importance of $CD8^+$ T-cell terminal differentiation in cytotoxic function [10].

Disease occurrence depends on a plethora of factors, including hormonal regulation of immune cells, which could shape infection outcome. Among hormonal effects on the immune response, glucocorticoids can promote a Th2 cytokine acquisition profile [14], facilitating Th2 activities, whereas its natural antagonist dehydroepiandrosterone (DHEA) is able to favor Th1 cytokine production and interfere with Th2 cytokine synthesis [15]. In fact, the synthetic DHEA derivative, 16 α-bromoepiandrosterone, exerts beneficial effects in clinical and experimental TB and in HIV patients [16–18]. We have previously demonstrated that in vitro treatment of PBMCs from HIV–TB patients with DHEA increased *Mtb*-specific IFN-γ responses and decreased FoxP3 expression in regulatory T cells, thus inducing a bias toward a protective antitubercular immune response [19].

Therefore, we aimed to study *Mtb*-specific cytotoxicity, IFN-γ secretion, and effector/memory differentiation of $CD8^+$T cells during HIV–TB coinfection and their modulation by adrenal hormones, focusing on DHEA effects. Our data show that HIV–TB coinfection is associated with both impaired cytotoxic *Mtb*-specific $CD8^+$ T-cell responses and irregular $CD8^+$ T-cell differentiation, the latter evidenced by lower CD45RA expression levels in T_{TE} $CD8^+$T cells and higher PD1 expression restricted to $CD27^+$ $CD8^+$T cells. Additionally, in vitro DHEA treatment enhanced *Mtb*-specific $CD8^+$ T-cell cytotoxic responses and $CD8^+$ T-cell terminal differentiation in HIV–TB. We propose that DHEA may contribute to improving antitubercular immunity by enhancing $CD8^+$ T-cell functions in HIV–TB patients.

Results

Functional subset distribution among peripheral $CD8^+$T cells in HIV–TB, HIV–LTB, HIV^+, and HD

In response to antigens, naïve $CD8^+$T cells (T_N) proliferate and differentiate into effector cells, which can be defined into at least three phenotypic groups according to their surface marker expression (reviewed in [10]). We analyzed bulk $CD8^+$ T-cell differentiation based on the expression of CD27 and CD45RA surface proteins as depicted in Fig. 1 [20–23]. HIV-infected patients with active TB (HIV–TB) or latent TB (HIV–LTB) and HIV^+ patients with no *Mtb* coinfection (HIV^+) displayed different subset distributions in total peripheral $CD8^+$T cells compared to healthy donors (HD) (Fig. 1A, pies). Moreover, both HIV–TB and HIV–LTB patients showed lower T_N but only HIV–TB patients showed higher T_{EM} and T_{TE} frequencies in total $CD8^+$T cells than HD (Fig. 1A, lower panel and B). Additionally, both HIV–TB and HIV–LTB patients exhibited a higher T_{TE}/T_N ratio compared to HD (Fig. 1C), thus indicating a shift to terminal differentiation among total $CD8^+$T cells in coinfected patients. These results are in line with the effect of *Mtb* infection on $CD8^+$ T-cell differentiation toward an effector phenotype proposed previously [11].

In order to establish whether the differences observed in circulating effector/memory subset proportions occurred due to alterations in the differentiation path, we evaluated transitions between effector/memory subsets by analyzing the correlation between phenotype proportions as described elsewhere [21, 24]. A statistically significant negative correlation between the proportions of two given subsets suggests that transitions between those populations are likely to occur. We observed a strong negative correlation between the percentage of T_{TE} and T_{EM} in bulk $CD8^+$T cells from HIV–TB individuals but not from HD (Fig. 1D). Although we also detected a significant negative correlation between the $\%T_{TE}$ and $\%T_{CM}$ (where T_{CM} is central memory T cells) in both groups (data not shown), such data suggest the occurrence of a distinct differentiation pattern induced by *Mtb* and/or HIV on total $CD8^+$T cells in coinfected patients that may account for the increment observed in T_{TE} proportions.

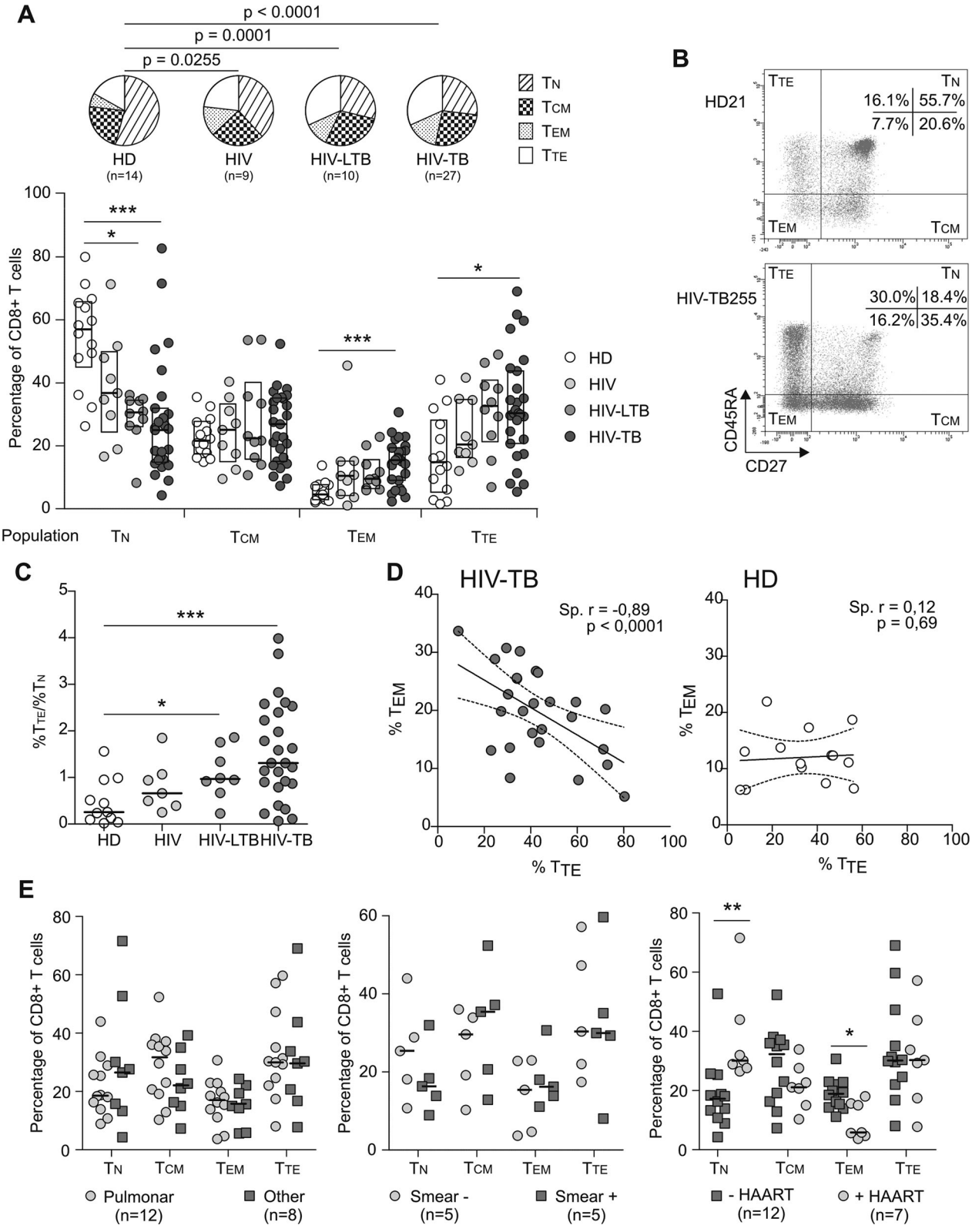

Extrapulmonary TB is more frequent among HIV-infected patients but the mechanisms of such increased incidence are not fully understood [25]. In order to better understand if the alterations observed in $CD8^+$ T-cell differentiation were related to TB localization or *Mtb* load, we stratified HIV–TB patients according to TB localization or smear test results (the latter associated with bacterial burden [11, 26]). However, we could not detect any differences in the proportions of bulk $CD8^+$ T-cell subsets among subgroups (Fig. 1E, left and middle panels). Interestingly, highly active antiretroviral therapy significantly changed effector/memory distribution in bulk $CD8^+$T cells ($p = 0.0349$ by partial permutation test) by reducing T_{EM} and augmenting T_N populations (Fig. 1E, right panel). This indicates a partial recovery of $CD8^+$T-cell homeostasis after anti-HIV treatment. Overall, these data indicate that HIV–TB coinfection induces a bias to terminal differentiation in total $CD8^+$T cells.

Effector/memory subsets phenotype in total $CD8^+$T cells from HIV–TB, HIV–LTB, HIV^+, and HD individuals

The CD45RA isoform of CD45 facilitates sustained T-cell receptor (TCR) signaling more efficiently than smaller isoforms like CD45R0, which contribute to the cessation of the immune response [27]. We observed a significantly lower relative intensity of CD45RA in T_{TE} $CD8^+$T cells in HIV–TB patients than HD (Fig. 2A and C). Additionally, despite the increment in $CD45RA^{hi}$ T_{TE} cells found in HIV–TB patients, $CD45RA^{dim}$ T_{TE} $CD8^+$T cells were increased remarkably both in HIV–TB and HIV–LTB patients compared to HD (Fig. 2B and C). This lower expression of CD45RA in bulk $CD8^+$ T_{TE} cells from HIV-*Mtb* coinfected patients may reduce responsiveness in these cells since CD45RA enhances TCR signaling [28, 29].

During HIV infection, PD-1 expression is a marker for abnormal naïve/memory distribution in T cells [30]. We observed an increment in PD1 expression on bulk $CD8^+$T cells among HIV–TB and HIV^+ patients compared to HD (Fig. 2D, left panel). Interestingly, PD-1 expression was mainly restricted to $CD27^+CD8^+$T cells in HIV–TB but not in HD (Fig. 2E). We also detected increased proportions of $CD27^{neg}CD8^+$T cells among HIV–TB compared to HD (Fig. 2D, right panel). Finally, we observed a positive correlation between the proportion of $PD1^+$ cells in $CD27^+CD8^+$T cells and the percentage of CD45RAdim T_{TE} in $CD8^+$T cells (Fig. 2F). These results suggest an association between increased proportions of not fully differentiated $CD8^+$T cells (in terms of CD45RA expression) and elevated percentages of exhausted $CD27^+CD8^+$T cells in HIV–TB patients. A higher expression of PD-1 in the $CD27^+$ population and a positive correlation between PD-1 expression on $CD27^+CD8^+$T cells and $CD45RA^{dim}$ cells in T_{TE} could imply an arrest of exhausted cells on a less differentiated and poor functional phenotype as observed in HIV^+ patients [31]. To sum up, these results suggest an impaired differentiation occurring concomitantly with an increased exhaustion of $CD8^+$T cells, both associated to HIV–TB coinfection.

Effect of in vitro Mtb stimulation on $CD8^+$T cells in HIV–TB subjects

We first observed that *Mtb*-induced degranulation and IFN-γ secretion in $CD8^+$T cells from HIV^+, HIV–LTB, or HIV–TB patients were not significantly different from media levels (Fig. 3A). In contrast, in vitro *Mtb* stimulation augmented both functions of $CD8^+$T cells in Bacillus Calmette Guérin (BCG)-vaccinated HD. This deficient *Mtb*-specific response in infected individuals did not occur due to a general impairment in $CD8^+$T cells reactivity since all the individuals tested responded to α-CD3/α-CD28 stimulation (Supporting Information Fig. 2).

In order to establish that *Mtb* in vitro stimulation induces terminal differentiation on total $CD8^+$T cells and whether this induction differs between HIV–TB patients and HD, we assessed effector/memory distribution before and after *Mtb* stimulation in both groups. Although we did not observe any changes in overall effector/memory distribution after *Mtb* stimulation in any of the groups (by partial permutation test, data not shown), we detected a slight but still significant increase in $CD8^+$ T_{TE} and T_{EM} populations and a reduction in T_N and T_{CM} populations in HD after Ag stimulation (Supporting Information Table 2). Conversely, *Mtb* stimulation did not induce any changes in T_{CM} populations among bulk $CD8^+$T cells in HIV–TB patients, but as observed in HD, it increased T_{EM} and T_{TE} cells and decreased T_N proportions.

Figure 1. Effector/memory phenotype and transitions in total peripheral CD8+T cells from HIV–TB, HIV^+, HIV-LTB and HD. Recently thawed or freshly isolated PBMCs were stained for the expression of CD45RA and CD27 in $CD8^+$T cells as described in *Methods*. (A–E) The expression of CD27 and CD45RA on $CD8^+$T cells from HD, HIV^+, HIV-LTB, and HIV–TB patients was analyzed by flow cytometry; (A, top) Pie charts summarize the data and each slice corresponds to the mean proportion of $CD8^+$T cells for each phenotype. (Bottom) Possible phenotypes are shown on the *x*-axis whereas percentages of distinct T-cell subsets within $CD8^+$T cells are shown on the *y*-axis. Comparisons of phenotype distribution were performed using the partial permutation test as described in [48] and the Kruskall–Wallis test followed by Dunn's multiple comparisons posttest. (B) Representative flow cytometry dot plot examples from an HD (top) and an HIV–TB patient (bottom). $CD8^+$T cells were gated as shown in Supporting information Fig. 1. (C) T_{TE}/T_{EM} ratio for each individual is shown. Comparisons were performed by the Kruskall–Wallis test followed by Dunn's multiple comparisons posttest. (D) Correlation analysis between the % T_{TE} and the %T_{EM} in $CD8^+$T cells were evaluated to assess recent effector/memory transitions as described previously [21, 24]. Figure shows %T_{TE} versus %T_{EM} in 27 HIV–TB (left) and 14 HD (right) subjects. Continuous lines represent linear regression curves and dashed lines represent 95% confidence intervals. Sp. *r*: Spearman's rank correlation coefficient. (E) Cumulative analyses of the expression of CD27 and CD45RA on $CD8^+$T cells from HIV–TB subjects stratified according to TB presentation (left), smear status (middle) and highly active antiretroviral therapy (HAART, right). Possible phenotypes are shown on the *x*-axis whereas percentages of distinct T-cell subsets within $CD8^+$T cells are shown on the *y*-axis. Comparisons of phenotype distribution were performed using the partial permutation test as described in [48] and the Kruskall–Wallis test followed by Dunn's multiple comparisons posttest. (A–E) Each symbol represents an individual subject (*n* values are shown in the figure). Horizontal lines represent median values and boxes represent interquartile range. $^*p < 0.05$; $^{**}p < 0.01$; $^{***}p < 0.001$.

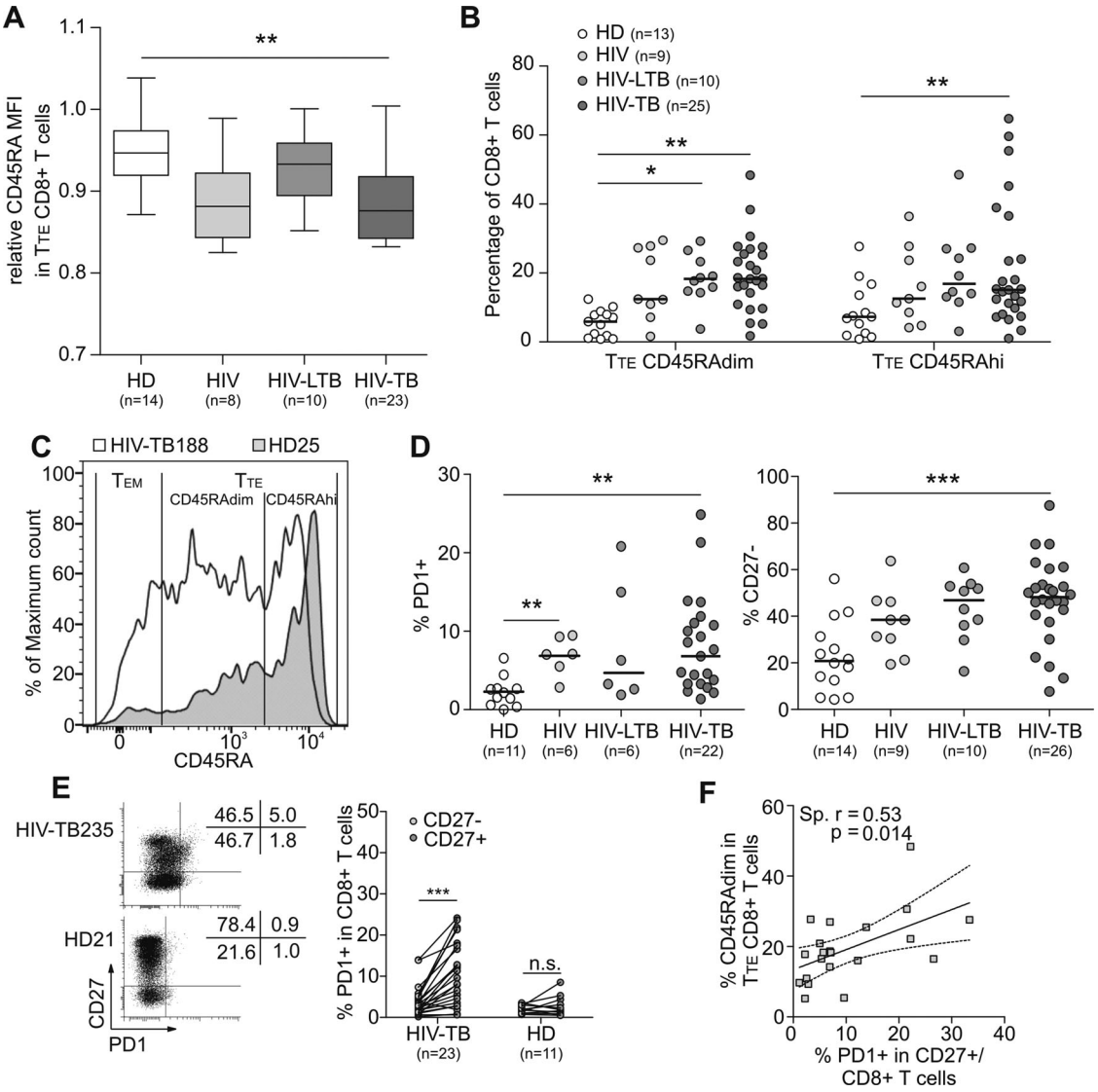

Figure 2. Phenotype of terminally differentiated CD8$^+$T cells in HIV–TB, HIV$^+$, HIV–LTB, and HD. Recently thawed or freshly isolated PBMCs were stained for CD27, CD45RA, and PD1 as described in *Methods* and analyzed by flow cytometry. (A) Analysis of the relative mean fluorescence intensity (MFI) of CD45RA in T_{TE} CD8$^+$T cells as defined by the ratio: [CD45RA MFI on T_{TE} / CD45RA MFI on T_N]. Horizontal lines represent median values, boxes represent interquartile ranges and whiskers represent 95% confidence intervals. (B, C) % of CD45RA^{dim} T_{TE} and CD45RA^{hi} T_{TE} among CD8$^+$T cells defined as described in Supporting Information Fig. 1. (C) Representative flow cytometry histogram examples showing the expression of CD45RA in CD27^{neg} CD8$^+$T cells from an HD (filled curve) and an HIV–TB patient (open curve). (D) Percentage of PD1$^+$ (left) and CD27^{neg} (right) cells among CD8$^+$T cells from HD ($n = 15$), HIV$^+$ ($n = 8$), HIV-LTB ($n = 10$) and HIV–TB ($n = 24$) subjects was determined by flow cytometry. (E, left) Representative dot plots for the expression of CD27 versus PD1 in total CD8$^+$T cells from an HIV–TB and an HD subject and cumulative analysis of PD1 expression in CD27^{neg} and CD27$^+$ CD8$^+$T cells from HIV–TB and HD (right). Each line connects the data for an individual patient. Comparisons between the CD27$^+$ and CD27^{neg} populations were performed using the Wilcoxon matched pairs test. (F) Correlation analysis between the %CD45RA^{dim} T_{TE} CD8$^+$ cells and %PD1 in CD27$^+$/CD8$^+$ cells in 23 HIV–TB patients. Continuous lines represent linear regression curves and dashed lines represent 95% confidence intervals. Sp. r: Spearman's rank coefficient. (B and D) Comparisons between groups were evaluated by the Kruskall–Wallis test followed by Dunn's multiple comparisons posttest. Horizontal lines represent median values, boxes represent interquartile ranges and whiskers represent 95% confidence intervals. Each symbol represents an individual subject. *N* values are shown in the figure. $^*p < 0.05$; $^{**}p < 0.01$; $^{***}p < 0.001$.

On the other hand, when analyzing *Mtb*-specific CD8$^+$T cells, different effector/memory distributions were observed between HD and HIV–TB for the three functions tested (Fig. 3B and C, pies). In HIV–TB patients, CD107a/b$^+$ and IFN-γ^+ CD8$^+$T cells showed higher T_{EM} and T_{TE} cells, respectively, while the three CD107a/b$^+$, IFN-γ^+, and bifunctional CD8$^+$T cells displayed lower T_N cells than HD (Fig. 3C, right panel). These results show that, as shown before for total CD8$^+$T cells, *Mtb*-specific CD8$^+$T cells in HIV–TB are biased to more differentiated stages independently of cell function.

Finally, correlation analyses were performed in order to ascertain transitions between populations in *Mtb*-specific CD8$^+$T cells, as described above, revealing a significantly negative correlation between the proportions of T_{TE} and T_{CM} among CD107a/b$^+$

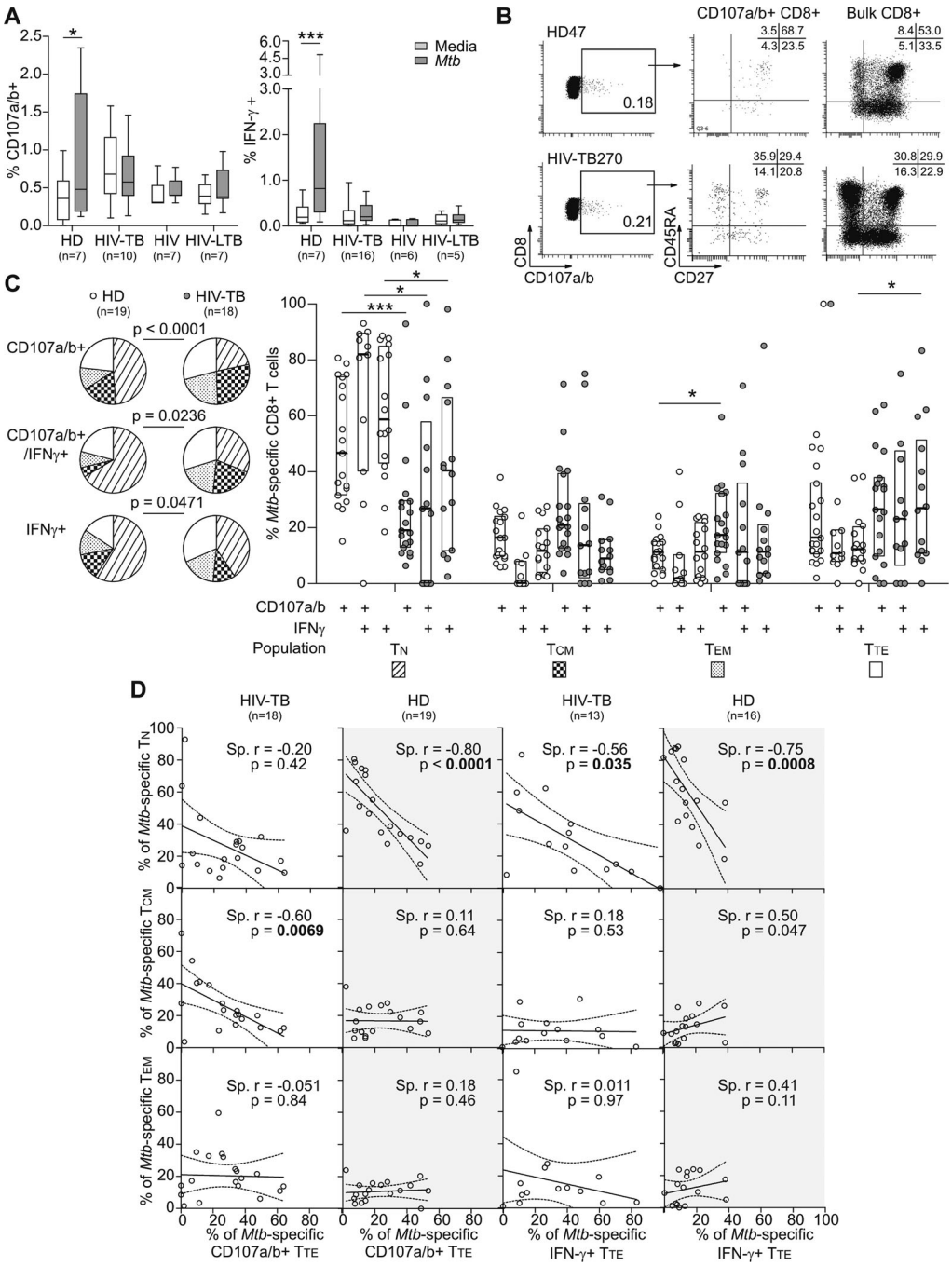

Figure 3. Effector/memory phenotype and transitions in Mtb-specific CD8$^+$T cells from HIV–TB patients and HD. (A) CD8$^+$T cells from HD, HIV$^+$, HIV-LTB, and HIV–TB individuals were in vitro stimulated and analyzed after 16 h for *Mtb*-induced CD107a/b and IFN-γ expression by flow cytometry. Comparisons between groups were performed using the Kruskall–Wallis test followed by Dunn's multiple comparisons posttest. (B–D) CD8$^+$T cells from HD and HIV–TB individuals were in vitro stimulated and analysed after 72 h for *Mtb*-induced CD107a/b, IFN-γ, CD27 and CD45RA expression by flow cytometry. CD8$^+$T cells were gated as shown in Supporting Information Fig. 1. The gating strategy is based on the distribution of CD27 and CD45RA on bulk CD8$^+$ T cells and it is then conserved in the analyses of CD107a/b$^+$ or IFN-γ$^+$ CD8$^+$ T cells. (B) Representative dot plots of the expression of CD107a/b$^+$ versus CD8 in CD8$^+$T cells (left), CD27 versus CD45RA in CD107a/b$^+$ CD8$^+$T cells (middle), and CD27 versus CD45RA in bulk CD8$^+$T cells (right) from an HD (top) and an HIV–TB patient (bottom). (C) Expression of CD27 and CD45RA on *Mtb*-specific CD8$^+$T cells from HD and HIV–TB individuals. (Left) Pie charts summarize the data and each slice corresponds to the mean proportion of *Mtb*-specific CD8$^+$T cells of each phenotype. (Right) Possible phenotypes are shown on the *x*-axis whereas percentages of distinct T-cell subsets within *Mtb*-specific CD8$^+$ T cells are shown on the y-axis. Comparisons of phenotype distribution were performed using the partial permutation test and the Kruskall–Wallis test followed by Dunn's multiple comparisons posttest. (D) Correlation analysis between the %T_{TE} and the %T_N, T_{CM}, or T_{EM} in CD107a/b$^+$ and IFN-γ$^+$ CD8$^+$T cells were evaluated in HIV–TB (white background) and HD (gray background) subjects. Continuous lines represent linear regression curves and dashed lines represent 95% confidence intervals. Sp. r: Spearman's rank coefficient. (A–D) Horizontal lines represent median values and boxes represent interquartile range. Each symbol represents an individual subject. *N* values are shown in the figure. * $p < 0.05$; ** $p < 0.01$; *** $p < 0.001$.

Mtb-specific CD8$^+$T cells in HIV–TB patients (Fig. 3D), which suggests a differentiation path from T_{CM} to T_{TE} in these cells. In contrast, CD107$^+$ CD8$^+$T cells from HD showed a significantly negative correlation between %T_{TE} and %T_N (Fig. 3D). Notably, IFN-γ-producing CD8$^+$T cells exhibited transitions from T_N to T_{TE} (Fig. 3D) in both groups. These observations indicate that effector/memory transitions in cytotoxic but not in IFN-γ secreting *Mtb*-specific CD8$^+$T cells are altered in HIV–TB patients.

Adrenal hormones and their interrelation with CD8$^+$T-cells subsets in HIV–TB

We have previously shown that HIV–TB coinfection is associated to lower DHEA plasma levels and higher cortisol/DHEA ratios [19]. Here, we aimed at establishing that the imbalance in adrenal hormone levels observed in HIV–TB patients was related to alterations in the CD8$^+$T-cell compartment. Therefore, we observed a positive correlation between DHEA plasma levels and the proportion of T_{TE} cells (Fig. 4A) or T_{TE} CD45RA^{hi} in bulk CD8$^+$T cells in HIV–TB patients but not in HIV$^+$, HIV–LTB (Fig. 4A), or HD (data not shown). Even though a lower number of subjects was analyzed in HIV and HIV–LTB groups, data trends suggest no association between DHEA plasma levels and CD8$^+$ T_{TE} or T_{TE} CD45RA^{dim} proportions in these groups. This lack of association would be in accordance with our previous observation of preserved DHEA levels in these patient groups [19]. No significant correlations were observed between DHEA plasma levels and the percentages of *Mtb*-specific CD8$^+$T cells or their effector/memory subsets in any of the groups studied (data not shown). Noteworthy, a strong positive correlation between *Mtb*-induced CD107a/b expression and cortisol plasma levels was observed in HIV–TB (Fig. 4B, left) but not in HD (Fig. 4B, middle). Interestingly, we did not find a similar correlation between cortisol plasma levels and HIV-specific CD8$^+$T cells in HIV$^+$ individuals (Fig. 4B, right), which suggests a unique adrenal imbalance related to the inflammation accompanying concomitant TB and HIV infections.

When analyzing the in vitro effect of DHEA on *Mtb*-specific CD8$^+$ T-cell cytotoxicity and IFN-γ responses in HIV–TB patients, we observed that the increment induced by DHEA treatment over *Mtb* responses positively correlated with CD4$^+$ T-cell counts (data not shown). Consistent with this, in those HIV–TB individuals with CD4$^+$ cell counts above 100 cells/μL, DHEA significantly increased *Mtb*-specific CD107a/b$^+$, IFN-γ, and bifunctional responses in CD8$^+$T cells (Fig. 4C). We did not observe any effects of DHEA on CD8$^+$ T-cell responses in those individuals with CD4$^+$ cell counts below 100 cell/μL (data not shown). These results indicate that, as shown previously [19], DHEA exerts its enhancer effect depending on the immune status of the individuals.

Effect of DHEA on CD8$^+$T-cell differentiation induced by Mtb stimulation

As the proportion of peripheral T_{TE} CD8$^+$T cells positively correlated with DHEA plasma levels in HIV–TB patients (Fig. 4A), we investigated the effect of DHEA addition over both effector/memory distribution and function of *Mtb*-stimulated CD8$^+$T cells. Even though DHEA treatment did not modify the overall effector/memory distribution of *Mtb*-specific CD8$^+$T cells (by partial permutation test, data not shown), in vitro DHEA treatment significantly increased T_{TE} CD107a/b$^+$ cells in *Mtb*-stimulated CD8$^+$T cells (Fig. 5A and B). We did not find any modulation on effector/memory subsets when analyzing IFN-γ-producing or bifunctional CD8$^+$T cells from HIV–TB individuals (Fig. 5A, middle and right panels, respectively). On the contrary, DHEA treatment did not modulate any subsets of *Mtb*-specific CD8$^+$T cells in HD (data not shown).

On the other hand, we analyzed the effect of in vitro DHEA treatment on the expression of transcription factors involved in CD8$^+$T-cell differentiation [32]. When coadministered with *Mtb,* DHEA treatment increased T-bet expression and T-bet/Eomesodermine (Eomes) ratio, both associated with terminal differentiation, in CD8$^+$ cells from HD (Fig. 5C and E, respectively). In contrast, *Mtb* stimulation alone increased Bcl-6 expression and reduced Blimp-1/Bcl-6 ratio (Fig. 5G and H, respectively), both associated with memory cell differentiation. Finally, DHEA also reverted the *Mtb*-induced decrease in Blimp-1/Bcl-6 ratio (Fig. 5H). Overall, these findings suggest that DHEA may bias *Mtb*-induced CD8$^+$T-cell differentiation toward an effector phenotype, probably through the increment in T-bet/Eomes ratio.

Effect of DHEA on in vitro Mtb-specific CD8$^+$T-cell responses

It has been proposed that the IFN-γ secreted by CD8$^+$T cells could enhance their cytolitic potential through macrophage activation [33]. Therefore, we analyzed the possible relationship between lytic degranulation and IFN-γ production in CD8$^+$T cells. While no significant correlation was observed between the percentages of CD107a/b$^+$ and IFN-γ$^+$ in CD8$^+$T cells from HIV–TB patients after in vitro *Mtb* stimulation (Fig. 6A), DHEA addition induced a positive correlation between both parameters (Fig. 6B). This positive correlation was similar to that observed when stimulating PBMCs from HIV–TB with Cytomegalovirus, Epstein–Barr, and influenza virus control peptide pool (CEF, Fig. 6C) or when stimulating PBMCs from HD with *Mtb* (Fig. 6D). Of note, CEF pool elicits responses against pathogens that, unlike HIV and *Mtb,* were either cleared (influenza) or controlled (CMV and Epstein-Barr). These results suggest that DHEA may at least partially restore the functional response of *Mtb*-specific CD8$^+$T lymphocytes in the context of HIV infection.

Discussion

Increasing experimental evidence over the past years has shown the relevance of CD8$^+$T cells on the antitubercular immune response [33]. The reduction in the frequency of CD8$^+$CCR7^{neg}CD45RA$^+$ T_{TE} cells and their granulysin content

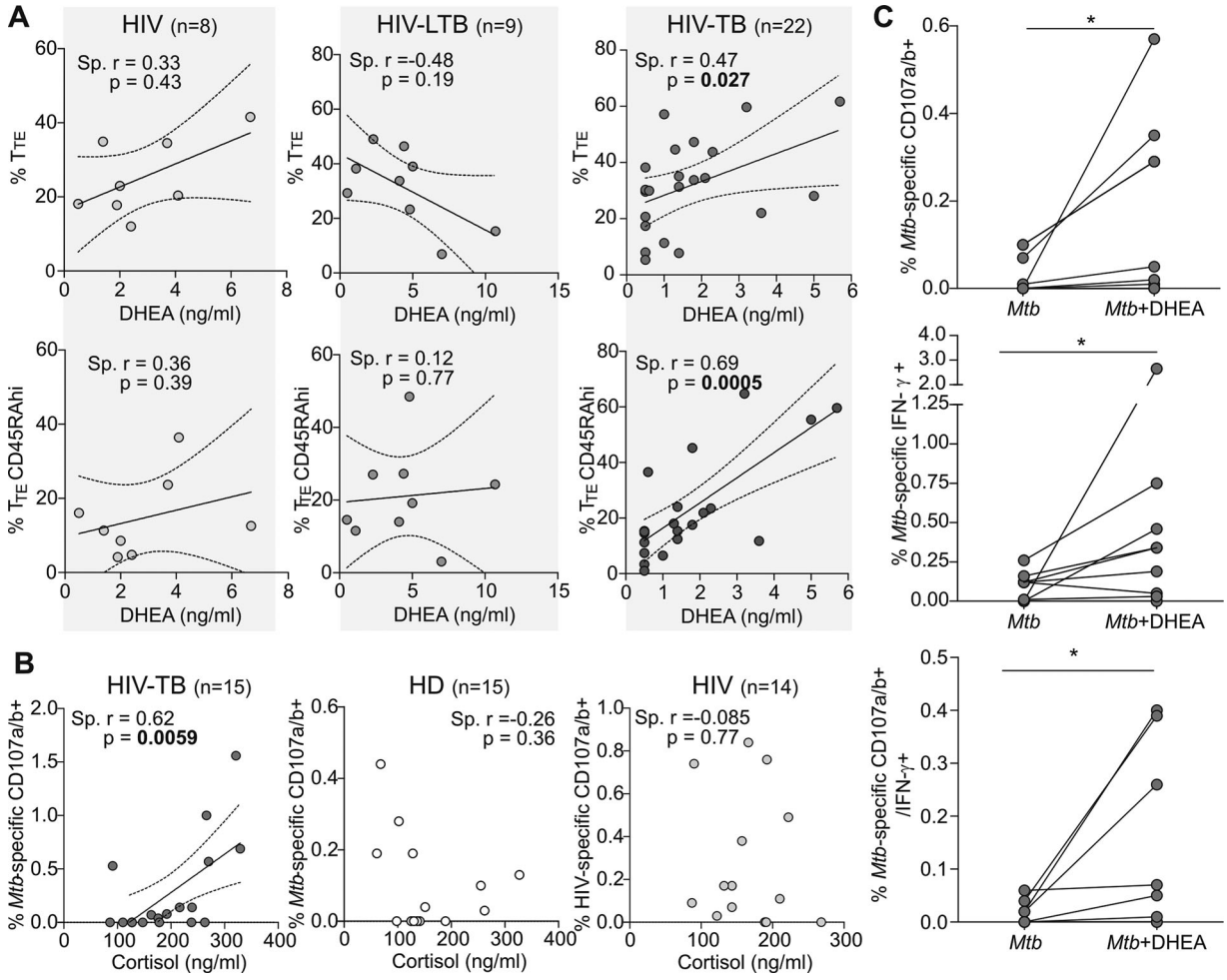

Figure 4. Adrenal hormone levels and their association with CD8$^+$T cells differentiation and function. (A) Recently thawed PBMCs were stained for the expression of CD45RA and CD27 and analyzed by flow cytometry. Plasma levels of DHEA were measured in the same blood samples as described in *Methods*. Figure shows correlation analyses between (top) the %T_{TE} or (bottom) T_{TE} CD45RA^{hi} in CD8$^+$T cells and DHEA plasma levels in (left) HIV$^+$, (middle) HIV-LTB, and (right) HIV–TB subjects. (B) PBMCs were incubated in the presence or absence of *Mtb* or HIV peptides and then the expression of CD107a/b, CD45RA, and CD27 were analyzed by flow cytometry. Plasma levels of cortisol were measured in the same blood samples as described in *Methods*. Figure shows correlation analysis between cortisol plasma levels and the percentage of *Mtb*-specific CD107a/b$^+$ CD8$^+$T cells in (left) HIV–TB and (middle) HD subjects or (right) the percentage of HIV-specific CD107a/b$^+$ CD8$^+$T cells in chronic HIV$^+$ subjects. (A, B) Values were media-subtracted and negative values were set to zero. Continuous lines represent linear regression curves and dashed lines represent 95% confidence intervals. Sp. r: Spearman's rank coefficient. Each symbol represents an individual subject. (C) PBMCs were incubated in the presence or absence of *Mtb* with or without DHEA and then the expression of CD107a/b and IFN-γ was evaluated in CD8$^+$T cells from 11 HIV–TB patients with CD4$^+$ T-cell counts higher than 100 cells/μL. Values were media-subtracted and negative values were set to zero. Each line connects the data for an individual patient. Comparisons between treatments were performed using the Wilcoxon matched pairs test. $^*p < 0.05$.

induced by anti-TNF-α immune therapy, a treatment known to dramatically increase TB reactivation in LTB patients, unraveled a critical role for these cells in maintaining latency and antimicrobial activity in *Mtb*-infected patients [9]. In this regard, we observed a bias to a more differentiated phenotype in total CD8$^+$T cells in HIV–TB patients, probably in an attempt to develop a more efficient antituberculous response. Also, contrary to HD, T_{TE} cells derived from both T_{EM} and T_{CM} populations in HIV–TB individuals (see Fig. 1C), which could contribute to the increased T_{TE} proportions observed in these patients. However, we observed lower levels of CD45RA on CD8$^+$T cells in HIV–TB patients, compared to HD, that may reflect a lower cell responsiveness, since an enhancing role for CD45RA in TCR signaling in multiple sclerosis and in the human cell line Jurkat has been described [27–29]. Similarly, HIV infection induces a maturation defect on HIV-specific T_{TE} cells, which may represent an HIV-induced evasion mechanism [34].

It is widely accepted that PD-1 reflects T-cell exhaustion in the context of chronic infections such as HIV and TB [30, 35]. Our results also demonstrate that PD-1 levels are increased among CD27$^+$CD8$^+$T cells in HIV–TB patients, providing new evidence pointing to an exhausted phenotype restricted to those cells that home to lymph nodes. These results are in line with the association of PD1 expression to a T-bet^{low}/Eomes^{hi} transitional memory phenotype in CD8$^+$T cells from HIV$^+$ patients observed by Buggert et al. [31]. Strikingly, our observation of a positive correlation between PD-1 expression on CD27$^+$CD8$^+$T cells (a

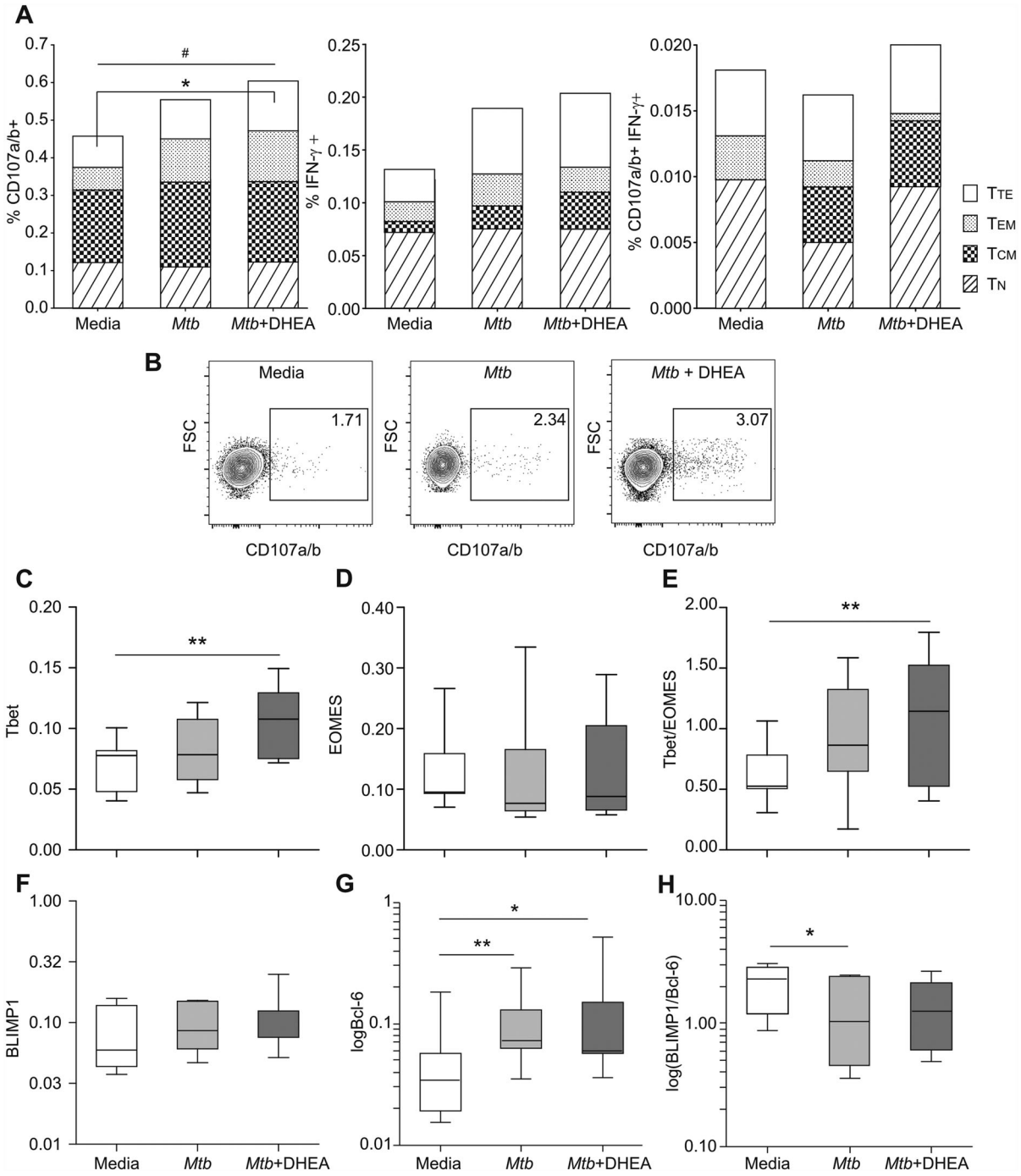

Figure 5. DHEA effect on Mtb-specific responses and terminal differentiation in $CD8^+$T cells from HIV–TB patients. (A, B) PBMCs from HIV–TB patients were stimulated with *Mtb* or *Mtb* supplemented with DHEA for 72 h and CD107a/b, IFN-γ, CD27, and CD45RA expression was analyzed by flow cytometry. (A, left) Frequencies of $CD107a/b^+$ ($n = 17$), (middle) IFN-γ^+ ($n = 11$), or (right) bifunctional $CD107a/b^+$/IFN-γ^+ ($n = 13$) T_N, T_{EM}, T_{CM}, and T_{TE} cells among $CD8^+$T cells from HIV–TB patients under basal conditions or after stimulation with *Mtb* or *Mtb* supplemented with DHEA. Bars represent the median value for each phenotype. $^*p < 0.05$ for $\%CD107^+$ T_{TE} cells in $CD8^+$T cells, $\#p < 0.05$ for $\%CD107^+$ cells in $CD8^+$T cells. (B) Representative dot plots showing the expression of CD107a/b versus FSC among T_{TE} $CD8^+$T cells from a representative HIV–TB patient in basal conditions (Media) or after stimulation with *Mtb* or *Mtb* + DHEA. (C–H) PBMCs from HD subjects were stimulated with *Mtb* or *Mtb* supplemented with DHEA for 72 h. Then, $CD8^+$ cells were isolated by positive selection and mRNA expression of the indicated molecules and GAPDH were determined by real time PCR. Figures show the relative expression to GAPDH of (C) Tbx-21 (T-bet), (D) Eomes, (F) Blimp-1 (G) BCL-6 mRNAs and (E) T-bet/Eomes or (H) Blimp-1/BCL-6 mRNA ratios in isolated $CD8^+$ cells from HD under basal conditions or after stimulation with *Mtb* or *Mtb* supplemented with DHEA. Horizontal lines represent median values, boxes represent interquartile ranges and whiskers represent 95% confidence intervals of seven donors from three independent experiments. (A–H) Comparisons between treatments were performed using the Kruskall–Wallis test followed by Dunns multiple comparisons posttest. $^*p < 0.05$, $^{**}p < 0.01$.

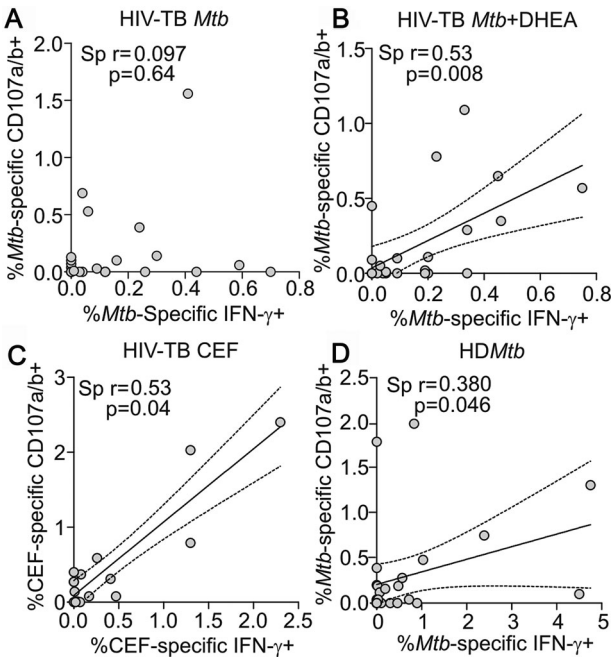

Figure 6. Correlation analysis between lytic degranulation and IFN-γ production in $CD8^+$T cells from HIV–TB patients. PBMCs from HD or HIV–TB patients were incubated under basal conditions or in the presence of *Mtb*, *Mtb* supplemented with DHEA or cytomegalovirus, Epstein–Barr, and influenza virus control peptide pool (CEF) and then the expression of CD107a/b and IFN-γ in $CD8^+$T cells was evaluated by flow cytometry. Figures show the correlation analyses between the %CD107a/b^+ and the %IFN-γ^+ cells among $CD8^+$T cells from HIV–TB subjects stimulated with (A) *Mtb* ($n = 31$), (B) *Mtb* + DHEA ($n = 30$), or (C) CEF ($n = 20$) and (D) among $CD8^+$T cells from HD subjects stimulated with *Mtb* ($n = 29$). Values were media-subtracted and negative values were set to zero. Each point represents an individual subject. Continuous lines represent linear regression curves and dashed lines represent 5–95% confidence intervals. Sp r: Spearman's rank coefficient.

population that includes T_N, T_{CM}, and transitional memory cells) and % $CD45RA^{dim}$ cells in T_{TE} points to an arrest of exhausted cells on less functional phenotypes as observed in HIV^+ patients [31].

Several authors have explored the dynamics of *Mtb*-specific $CD4^+$T cells but just a few studies have been focused on *Mtb*-specific $CD8^+$T cells. However, to our knowledge, only three studies described *Mtb*-specific $CD8^+$T cells in the context of HIV coinfection [12, 13, 36]. At present, this is the first report addressing *Mtb*-specific cytotoxic $CD8^+$ T-cell responses and their memory status in HIV–TB coinfected patients. In TB patients, Rozot et al. ascertained that *Mtb*-specific $CD8^+$T cells were mostly T_{EM} cells [11]. On the other hand, Caccamo et al. studied the phenotype of *Mtb*-specific $CD8^+$T cells by tetramer staining in TB patients, and observed a predominance of T_{CM} and lower T_{TE} $CD8^+$T cells, both of which were reverted after anti-TB therapy [37]. Lastly, Chiacchio et al. observed higher *Mtb*-specific T_{TE} $CD8^+$T cells in HIV–LTB individuals, but not in HIV–TB patients [12].

Contrary to those data, we detected elevated levels of T_{TE} and T_{EM} $CD8^+$T cells in *Mtb*-specific IFN-γ+ and CD107a/b^+ cells, respectively, in HIV–TB compared to HD. These differences may be linked to the use of distinct stimuli and/or markers to define *Mtb*-specific and memory/effector populations but it is likely that HIV infection and its related alterations in the immune system homeostasis induce changes in *Mtb*-specific $CD8^+$T-cell differentiation.

We also found that *Mtb*-specific CD107a/b^+ $CD8^+$T cells were fueled by T_{CM} in HIV–TB, whereas in HD, they originated mainly from T_N. On the contrary, IFN-γ+ T_{TE} originated from T_N both in HIV–TB and HD. These analyses show for the first time not only maturation but also cell transition differences depending on cell function during HIV–TB coinfection.

Endocrine hormones, and particularly adrenal hormones such as DHEA, are prone to modulate immune functions during HIV–TB coinfection as described previously by our group [19]. According to this, the present study shows that DHEA enhances $CD8^+$ T-cell responses and terminal differentiation (Fig. 4A and 5A) in HIV–TB coinfected individuals, suggesting a protective role for DHEA against mycobacteria in these patients. Even though DHEA can directly increase $CD8^+$ T-cell responses as shown by our in vitro experiments, we did not find any correlation between DHEA plasma levels and the percentage of *Mtb*-specific $CD8^+$T cells. As the amount of DHEA in plasma and the intensity of the immune response to *Mtb* are determined by several factors (i.e. activation of hypothalamus–pituitary axis [14], TB burden [38], or HIV disease progression [25], among others), the association between DHEA plasma levels and *Mtb*-specific $CD8^+$T cells proportions in our cohort could be masked by these other factors.

Contrary to our expectations, we detected a positive correlation between cortisol plasma levels and CD107a/b^+ $CD8^+$T cells in HIV–TB individuals (Fig. 4B). We propose that *Mtb* infection may induce an increment in cortisol levels while concomitantly increasing *Mtb*-specific $CD8^+$ T-cell responses, driving to the observed association. These findings may be interpreted as an attempt of the endocrine system to modulate the inflammation induced by both infections.

In the present study, we observed that DHEA plasma levels positively correlated with T_{TE} and, importantly, $CD45RA^{hi}$ T_{TE} proportions in $CD8^+$T cells, and in vitro DHEA increased cytotoxic T_{TE} $CD8^+$T cells and diverted the $CD8^+$ cell transcriptional profile to a terminal effector one. Since macrophage activation by IFN-γ increases antigen presentation [39], one can expect a direct association between *Mtb*-specific IFN-γ and cytotoxic responses [40]. Our results show that, contrary to HD, the above-mentioned association is impaired in HIV–TB patients and, more important, that in vitro DHEA treatment could restore the positive correlation between *Mtb*-specific degranulating and IFN-γ- producing $CD8^+$T cells in HIV–TB patients. The latter results point to an indirect effect of DHEA on $CD8^+$T cells through antigen-presenting cells. Accordingly, we previously observed that DHEA improved the production of IL-12 and the antigen-specific T-cell responses induced by *Mtb*-stimulated dendritic cells [41]. Also, during *Lysteria monocytogenes* infection, IL-12 represses Eomes and enhances T-bet in effector $CD8^+$T cells, while after the resolution of infection and abatement of IL-12 signaling, Eomes expression rises whereas T-bet expression declines in memory $CD8^+$T cells [42]. Therefore, the effect of DHEA on $CD8^+$T-cell differentiation and IFN-γ and

cytotoxic responses may be mediated by an enhancement on IL-12 production as shown previously [42].

To date, this is the first report showing an in-depth analysis of the $CD8^+$ T-cell memory/effector phenotype in HIV–TB coinfected patients and its modulation by DHEA, paving the way for delineating novel approaches for a better management of *Mtb* infection in people living with HIV.

Methods

Patients

The present study has a cross-sectional design. Patients were evaluated at Hospital J.A. Fernández, Buenos Aires (Table 1). Groups: HIV^+: tuberculin skin test negative, chronically HIV-1^+ infected patients as determined by ELISA and confirmatory Western blot; HIV–LTB: HIV-1^+ individuals with latent TB as determined by tuberculin skin test; HIV–TB: HIV-1^+ patients with active TB and less than 1 week of anti-TB therapy and HD: HD with no history of TB contact. Diagnosis of TB was based on the identification of acid-fast bacilli in sputum, a positive culture of TB bacilli and clinical and/or radiological data. All individuals were BCG vaccinated. None of the recruited individuals received DHEA or glucocorticoid treatment. Some HIV-1 infected individuals were on antiretroviral treatment following current guidelines [43]. The Ethics Committee from Fundación Huésped approved the current study. Written informed consent was documented from all study subjects.

Hormone assessment

EDTA-anticoagulated blood samples were drawn during morning hours. Plasma cortisol was measured by automated electrochemiluminescence immunoassay (Roche Diagnostics GmbH) and DHEA by radioimmunoassay (IMMUNOTECH) following manufacturer's instructions.

Antigens

Pretitrated *Mtb* H37Rv, gamma-irradiated whole cells (NR-14819, BEI Resources, NIAID, NIH) was used at 10 μg/mL final concentration. Cytomegalovirus, Epstein–Barr, and influenza virus control peptide pool (CEF) was obtained from the NIH AIDS Reagent Program, Division of AIDS, NIAID, NIH. Lyophilized peptides were dissolved in dimethyl sulfoxide at 20 μg/μL and stored at −20°C.

Culture conditions

PBMCs were isolated by density gradient centrifugation on Ficoll–Hypaque and cultured at 2×10^6 cells/mL with *Mtb* (10 μg/mL), CEF (2 μg/mL), or anti-CD3 (10 ng/mL) and anti-CD28 (1 μg/mL) antibodies in 48-well plates with RPMI medium (Sigma-Aldrich) supplemented with 10% fetal bovine serum (PAA), 2 mM L-glutamine (Gibco BRL), 100 U/mL penicillin (PAA) and 100 mg/mL streptomycin (Gibco BRL), in the presence or absence of DHEA (Sigma-Aldrich, 10^{-7} M). After 16 or 72 h, cells were harvested, stained, and analyzed by flow cytometry or $CD8^+$ cells were isolated and lysed as described below.

Flow cytometry

PBMCs were stained for CD3, CD8, CD27, CD45RA, and PD-1 expression using specific mAbs (Biolegend). In some experiments, cultured PBMCs were surface stained for CD3, CD8, CD27, and CD45RA; concomitantly, intracellular cytokine staining was performed to determine IFN-γ production as described elswhere [44, 45] and CD107a/b expression was determined (20 μL/mL; BDBiosciences) to measure $CD8^+$T lymphocyte cytotoxic degranulation as described previously [46]. Negative control samples were incubated with irrelevant, isotype-matched mAbs in parallel with experimental samples. Dead cells were excluded by using Live/Dead (Life Technologies) viability probe following manufacturer's instructions. Samples acquisition and analysis were carried out on a FACSCanto flow cytometer using the BD FACSDiva software (BD Biosciences).

Real-time PCR

$CD8^+$ cells were isolated by positive selection using CD8 magnetic beads (BD Biosciences), and then harvested in Trizol Reagent (Invitrogen) following manufacturer's instructions. Afterwards, total RNA was quantified by 260 nm absorbance and cDNA was synthesized by MMLV retrotranscription (Invitrogen) following manufacturer's instructions. Real Time PCR was performed using

Table 1. Epidemiological characteristics of the subjects enrolled

	HIV–TB	HIV–LTB	HIV	HD
Number of subjects enrolled	47	11	12	25
Median age in years (IQR)	38 (31–43)	35 (28–40)	35 (32–48)	36 (30–46)
Female/male distribution	21/26	3/8	3/9	16/9
HIV status	+	+	+	–
Median CD4 count (IQR)	93 (37-213)	361 (261–650)	286 (141–452)	843 (607–1075)
Median Viral Load (IQR)	39 867 (3789–160 732)	12 934 (756–24 590)	11 225 (25–36 581)	–

IQR, Interquartile range.

CyberGreen Select (Invitrogen) in a 7500 Real-Time PCR (Applied Biosystems) to determine the relative expression of the genes depicted in Table 1 from Supporting Information. Data analysis was performed using LinRegPCR software [47].

Statistical analysis

Statistical analyses were conducted using GraphPad Prism 5 version 5.04. Comparisons between groups were evaluated by the Kruskall–Wallis analysis of variance followed by post hoc comparisons (Dunn's test) when applicable. Paired sample comparisons were performed using the non-parametric Wilcoxon matched pairs test. Correlations were determined using Spearman's rank test. Statistical analysis and display of multicomponent distributions were performed by partial permutation test using SPICE v5.1 (http://exon.niaid.nih.gov/spice/) [48]. p values below 0.05 were considered significant.

Acknowledgments: We thank the study subjects for their participation, Federico Remes Lenicov and Silvia de la Barrera for continuous support, Sergio Mazzini for revising the manuscript, Graciela Ben for assistance in recruiting the patients and Diego Gonzalez for assistance in hormone assessment. This work was supported by Agencia Nacional de Promoción Científica y Tecnológica (PICT 2010-0656 and PICT 2012-0059 M.F.Q.), University of Buenos Aires (UBACyT 20020120200050BA M.F.Q.) and Consejo Nacional de Investigaciones Científicas y Técnicas (CONICET, PIP 0010 M.F.Q.).

Conflict of interest: The authors declare no commercial or financial conflict of interest.

References

1 **Getahun, H., Gunneberg, C., Granich, R. and Nunn, P.**, HIV infection-associated tuberculosis: the epidemiology and the response. *Clin. Infect. Dis.* 2010. **50**(Suppl 3): S201–S207.

2 **Kaufmann, S. H., Cole, S. T., Mizrahi, V., Rubin, E. and Nathan, C.**, Mycobacterium tuberculosis and the host response. *J. Exp. Med.* 2005. **201**: 1693–1697.

3 **Rahman, S., Gudetta, B., Fink, J., Granath, A., Ashenafi, S., Aseffa, A., Derbew, M. et al.**, Compartmentalization of immune responses in human tuberculosis: few CD8+ effector T cells but elevated levels of FoxP3+ regulatory t cells in the granulomatous lesions. *Am. J. Pathol.* 2009. **174**: 2211–2224.

4 **van Pinxteren, L. A., Cassidy, J. P., Smedegaard, B. H., Agger, E. M. and Andersen, P.**, Control of latent Mycobacterium tuberculosis infection is dependent on CD8 T cells. *Eur. J. Immunol.* 2000. **30**: 3689–3698.

5 **Lewinsohn, D. A., Heinzel, A. S., Gardner, J. M., Zhu, L., Alderson, M. R. and Lewinsohn, D. M.**, Mycobacterium tuberculosis-specific CD8+ T cells preferentially recognize heavily infected cells. *Am. J. Respir. Crit. Care Med.* 2003. **168**: 1346–1352.

6 **Harty, J. T., Tvinnereim, A. R. and White, D. W.**, CD8+ T cell effector mechanisms in resistance to infection. *Annu. Rev. Immunol.* 2000. **18**: 275–308.

7 **Stenger, S., Mazzaccaro, R. J., Uyemura, K., Cho, S., Barnes, P. F., Rosat, J. P., Sette, A. et al.**, Differential effects of cytolytic T cell subsets on intracellular infection. *Science* 1997. **276**: 1684–1687.

8 **Woodworth, J. S., Wu, Y. and Behar, S. M.**, Mycobacterium tuberculosis-specific CD8+ T cells require perforin to kill target cells and provide protection in vivo. *J. Immunol.* 2008. **181**: 8595–8603.

9 **Bruns, H., Meinken, C., Schauenberg, P., Harter, G., Kern, P., Modlin, R. L., Antoni, C. et al.**, Anti-TNF immunotherapy reduces CD8+ T cell-mediated antimicrobial activity against Mycobacterium tuberculosis in humans. *J. Clin. Invest.* 2009. **119**: 1167–1177.

10 **Mahnke, Y. D., Brodie, T. M., Sallusto, F., Roederer, M. and Lugli, E.**, The who's who of T-cell differentiation: human memory T-cell subsets. *Eur. J. Immunol.* 2013. **43**: 2797–2809.

11 **Rozot, V., Vigano, S., Mazza-Stalder, J., Idrizi, E., Day, C. L., Perreau, M., Lazor-Blanchet, C. et al.**, Mycobacterium tuberculosis-specific CD8+ T cells are functionally and phenotypically different between latent infection and active disease. *Eur. J. Immunol.* 2013. **43**: 1568–1577.

12 **Chiacchio, T., Petruccioli, E., Vanini, V., Cuzzi, G., Pinnetti, C., Sampaolesi, A., Antinori, A. et al.**, Polyfunctional T-cells and effector memory phenotype are associated with active TB in HIV-infected patients. *J. Infect.* 2014. **69**: 533–545.

13 **Ongaya, A., Huante, M. B., Mwangi, P., Keiser, P. H., Amukoye, E. and Endsley, J. J.**, Mycobacterium tuberculosis-specific CD8+ T cell recall in convalescing TB subjects with HIV co-infection. *Tuberculosis (Edinb)* 2013. **93**(Suppl): S60–S65.

14 **Bottasso, O., Bay, M. L., Besedovsky, H. and del Rey, A.**, The immuno-endocrine component in the pathogenesis of tuberculosis. *Scand. J. Immunol.* 2007. **66**: 166–175.

15 **Dillon, J. S.**, Dehydroepiandrosterone, dehydroepiandrosterone sulfate and related steroids: their role in inflammatory, allergic and immunological disorders. *Curr. Drug Targets Inflamm. Allergy* 2005. **4**: 377–385.

16 **Reading, C., Dowding, C., Schramm, B., Garsd, A., Onizuka-Handa, N., Stickney, D. and Frincke, J.**, Improvement in immune parameters and human immunodeficiency virus-1 viral response in individuals treated with 16alpha-bromoepiandrosterone (HE2000). *Clin. Microbiol. Infect.* 2006. **12**: 1082–1088.

17 **Stickney, D. R., Noveljic, Z., Garsd, A., Destiche, D. A. and Frincke, J. M.**, Safety and activity of the immune modulator HE2000 on the incidence of tuberculosis and other opportunistic infections in AIDS patients. *Antimicrob. Agents Chemother.* 2007. **51**: 2639–2641.

18 **Hernandez-Pando, R., Aguilar-Leon, D., Orozco, H., Serrano, A., Ahlem, C., Trauger, R., Schramm, B. et al.**, 16alpha-Bromoepiandrosterone restores T helper cell type 1 activity and accelerates chemotherapy-induced bacterial clearance in a model of progressive pulmonary tuberculosis. *J. Infect. Dis.* 2005. **191**: 299–306.

19 **Quiroga, M. F., Angerami, M. T., Santucci, N., Ameri, D., Francos, J. L., Wallach, J., Sued, O. et al.**, Dynamics of adrenal steroids are related to variations in Th1 and Treg populations during Mycobacterium tuberculosis infection in HIV positive persons. *PLoS One* 2012. **7**: e33061.

20 **Hamann, D., Baars, P. A., Rep, M. H., Hooibrink, B., Kerkhof-Garde, S. R., Klein, M. R. and van Lier, R. A.**, Phenotypic and functional separation of memory and effector human CD8+ T cells. *J. Exp. Med.* 1997. **186**: 1407–1418.

21 **Mailloux, A. W., Sugimori, C., Komrokji, R. S., Yang, L., Maciejewski, J. P., Sekeres, M. A., Paquette, R. et al.**, Expansion of effector memory

regulatory T cells represents a novel prognostic factor in lower risk myelodysplastic syndrome. *J. Immunol.* 2012. **189**: 3198–3208.

22 **Khamesipour, A., Nateghi Rostami, M., Tasbihi, M., Miramin Mohammadi, A., Shahrestani, T., Sarrafnejad, A., Sohrabi, Y. et al.**, Phenotyping of circulating CD8(+) T cell subsets in human cutaneous leishmaniasis. *Microbes Infect.* 2012.

23 **Larbi, A. and Fulop, T.**, From "truly naive" to "exhausted senescent" T cells: when markers predict functionality. *Cytometry A* 2014. **85**: 25–35.

24 **Ghiglione, Y., Falivene, J., Ruiz, M. J., Laufer, N., Socias, M. E., Cahn, P., Giavedoni, L. et al.**, Early skewed distribution of total and HIV-specific CD8+ T-cell memory phenotypes during primary HIV infection is related to reduced antiviral activity and faster disease progression. *PLoS One* 2014. **9**: e104235.

25 **Gray, J. M. and Cohn, D. L.**, Tuberculosis and HIV coinfection. *Semin. Respir. Crit Care Med.* 2013. **34**: 32–43.

26 **Helke, K. L., Mankowski, J. L. and Manabe, Y. C.**, Animal models of cavitation in pulmonary tuberculosis. *Tuberculosis (Edinb)* 2006. **86**: 337–348.

27 **Rhee, I. and Veillette, A.**, Protein tyrosine phosphatases in lymphocyte activation and autoimmunity. *Nat. Immunol.* 2012. **13**: 439–447.

28 **Do, H. T., Baars, W., Borns, K., Windhagen, A. and Schwinzer, R.**, The 77C→G mutation in the human CD45 (PTPRC) gene leads to increased intensity of TCR signaling in T cell lines from healthy individuals and patients with multiple sclerosis. *J. Immunol.* 2006. **176**: 931–938.

29 **Wang, Y. and Johnson, P.**, Expression of CD45 lacking the catalytic protein tyrosine phosphatase domain modulates Lck phosphorylation and T cell activation. *J. Biol. Chem.* 2005. **280**: 14318–14324.

30 **Breton, G., Chomont, N., Takata, H., Fromentin, R., Ahlers, J., Filali-Mouhim, A., Riou, C. et al.**, Programmed death-1 is a marker for abnormal distribution of naive/memory T cell subsets in HIV-1 infection. *J. Immunol.* 2013. **191**: 2194–2204.

31 **Buggert, M., Tauriainen, J., Yamamoto, T., Frederiksen, J., Ivarsson, M. A., Michaelsson, J., Lund, O. et al.**, T-bet and Eomes are differentially linked to the exhausted phenotype of CD8+ T cells in HIV infection. *PLoS Pathog.* 2014. **10**: e1004251.

32 **Kaech, S. M. and Cui, W.**, Transcriptional control of effector and memory CD8+ T cell differentiation. *Nat. Rev. Immunol.* 2012. **12**: 749–761.

33 **Behar, S. M.**, Antigen-specific CD8(+) T cells and protective immunity to tuberculosis. *Adv. Exp. Med. Biol.* 2013. **783**: 141–163.

34 **Champagne, P., Ogg, G. S., King, A. S., Knabenhans, C., Ellefsen, K., Nobile, M., Appay, V. et al.**, Skewed maturation of memory HIV-specific CD8 T lymphocytes. *Nature* 2001. **410**: 106–111.

35 **Wallis, R. S., Kim, P., Cole, S., Hanna, D., Andrade, B. B., Maeurer, M., Schito, M. et al.**, Tuberculosis biomarkers discovery: developments, needs, and challenges. *Lancet Infect. Dis.* 2013. **13**: 362–372.

36 **Shao, L., Zhang, W., Zhang, S., Chen, C. Y., Jiang, W., Xu, Y., Meng, C. et al.**, Potent immune responses of Ag-specific Vgamma2Vdelta2+ T cells and CD8+ T cells associated with latent stage of Mycobacterium tuberculosis coinfection in HIV-1-infected humans. *Aids* 2008. **22**: 2241–2250.

37 **Caccamo, N., Meraviglia, S., La Mendola, C., Guggino, G., Dieli, F. and Salerno, A.**, Phenotypical and functional analysis of memory and effector human CD8 T cells specific for mycobacterial antigens. *J. Immunol.* 2006. **177**: 1780–1785.

38 **Mattila, J. T., Diedrich, C. R., Lin, P. L., Phuah, J. and Flynn, J. L.**, Simian immunodeficiency virus-induced changes in T cell cytokine responses in cynomolgus macaques with latent Mycobacterium tuberculosis infection are associated with timing of reactivation. *J. Immunol.* 2011. **186**: 3527–3537.

39 **Zhou, F.**, Molecular mechanisms of IFN-gamma to up-regulate MHC class I antigen processing and presentation. *Int. Rev. Immunol* .2009. **28**: 239–260.

40 **Woodworth, J. S. and Behar, S. M.**, Mycobacterium tuberculosis-specific CD8+ T cells and their role in immunity. *Crit. Rev. Immunol.* 2006. **26**: 317–352.

41 **Angerami, M., Suarez, G., Pascutti, M. F., Salomon, H., Bottasso, O. and Quiroga, M. F.**, Modulation of the phenotype and function of Mycobacterium tuberculosis-stimulated dendritic cells by adrenal steroids. *Int. Immunol.* 2013. **25**: 405–411.

42 **Takemoto, N., Intlekofer, A. M., Northrup, J. T., Wherry, E. J. and Reiner, S. L.**, Cutting Edge: IL-12 inversely regulates T-bet and eomesodermin expression during pathogen-induced CD8+ T cell differentiation. *J. Immunol.* 2006. **177**: 7515–7519.

43 Panel on Antiretroviral Guidelines for Adults and Adolescents. Guidelines for the use of antiretroviral agents in HIV-1-infected adults and adolescents. Department of Health and Human Services. Available at http://www.aidsinfo.nih.gov/ContentFiles/AdultandAdolescentGL.pdf. Accessed January 2015.

44 **Quiroga, M. F., Pasquinelli, V., Martinez, G. J., Jurado, J. O., Zorrilla, L. C., Musella, R. M., Abbate, E. et al.**, Inducible costimulator: a modulator of IFN-gamma production in human tuberculosis. *J. Immunol.* 2006. **176**: 5965–5974.

45 **Quiroga, M. F., Jurado, J. O., Martinez, G. J., Pasquinelli, V., Musella, R. M., Abbate, E., Issekutz, A. C. et al.**, Cross-talk between CD31 and the signaling lymphocytic activation molecule-associated protein during interferon- gamma production against Mycobacterium tuberculosis. *J. Infect. Dis.* 2007. **196**: 1369–1378.

46 **Betts, M. R., Brenchley, J. M., Price, D. A., De Rosa, S. C., Douek, D. C., Roederer, M. and Koup, R. A.**, Sensitive and viable identification of antigen-specific CD8+ T cells by a flow cytometric assay for degranulation. *J. Immunol. Methods* 2003. **281**: 65–78.

47 **Ruijter, J. M., Ramakers, C., Hoogaars, W. M., Karlen, Y., Bakker, O., van den Hoff, M. J. and Moorman, A. F.**, Amplification efficiency: linking baseline and bias in the analysis of quantitative PCR data. *Nucleic Acids Res.* 2009. **37**: e45.

48 **Roederer, M., Nozzi, J. L. and Nason, M. C.**, SPICE: exploration and analysis of post-cytometric complex multivariate datasets. *Cytometry A* 2011. **79**: 167–174.

Abbreviations: **BCG**: Bacillus Calmette Guérin · **DHEA**: dehydroepiandrosterone · **HD**: healthy donor · **LTB**: latent tuberculosis infection · **MFI**: mean fluorescence intensity · ***Mtb***: *Mycobacterium tuberculosis* · **TB**: tuberculosis · T_{CM}: central memory T cells · T_{EM}: effector memory T cells · T_N: naïve T cells · T_{TE}: terminal effector T cells · **TCR**: T cell receptor

Full correspondence: Guadalupe V. Suarez, Instituto de Investigaciones Biomédicas en Retrovirus y SIDA, University of Buenos Aires, Paraguay 2155 P.11, Capital Federal, C1121ABG Buenos Aires, Argentina
Fax: 54-11-4508-3705
e-mail: suarez_guadalupe@hotmail.com

Received: 2/2/2015
Revised: 8/5/2015
Accepted: 1/6/2015
Accepted article online: 5/6/2015

